Design of Anti-interference System for Fully Autonomous UAV Based on ADRC-EKF Algorithm

Liang Lin[a], Chengbin Chen[*,a], Kaixiong Su, Baihe Chen, Hanwen Li
College of Physics and Information Engineering
Fuzhou University
Fuzhou, China
[a] Authors equally contributed to the work
*Corresponding author
e-mail: 385697936@qq.com

***Abstract*—In order to solve the short-time drift problem of height data caused by environmental and noisy pollution, a multi-rotor aircraft control system was designed to prevent the aircraft from falling rapidly in a short time during the autonomous cruise. The problem of data loss due to strong interference on the UAV, which is equipped with the Real-time kinematic (RTK), can be well solved by introducing an inertial measurement unit (IMU) for high resolution, and using an Extended Kalman filter and IMU to calculate system acceleration (ACC) as well as altitude predictions for eliminating height drift due to sensor errors. In addition, the ADRC control algorithm is also introduced to control the attitude of the aircraft, to realize the control compensation, and finally to control the height of the drone through the three-ring cascade PID algorithm. The experimental results show that the proposed algorithm can make the UAV get better height and attitude control even though the external disturbance is unknown.**

Keywords-extended Kalman filter; ADRC; attitude control algorithm

I. INTRODUCTION

Due to the light weight and low cost of drones, the application scenarios have become more and more extensive [1-4]. However, there are still some problems to be solved in practical application of the drones. Most outdoor cruising drones use global positioning systems (GPS) to provide location data, but the GPS signals are susceptible in the wild and complex electromagnetic environments. Therefore, it is necessary to propose an attitude and altitude control algorithm for UAVs against electromagnetic interference and environmental noise.

Nowadays, the widely used methods to control the high-precision height of UAV are adopting the RTK reads the absolute position information of centimeter-level in the inertial coordinate system and using cascade PID control algorithm and the Extended Kalman filter algorithm control the taking-off and landing of the UAV [5]. However,due to the over dependence of the drones on the sensor, a data error will occur when the RTK is affected by strong interference, which will cause the aircraft to shake and affect the control performance. As far as we know, most researches are focusing on the UAV height measurement with high accuracy through multi-sensor fusion [6-7], but the dynamic performance of the drone during flight is ignored. According to the application, using a new type of near-ground sensor to improve the flight control performance is proposed. There are also proposals about setting a new type of near-ground sensor to improve the flight control performance. But various interference factors such as signals and terrain are neglected, which reduces the reliability of the sensor, and greatly increase the flight failure rate of the drone [8].

To solve above problems, in this paper we propose using EKF [9] to process data obtained by sensors such as IMU and barometer that are less susceptible to environmental changes during operation, to predict the altitude information of drones, and to improve the reliability of altitude measurement data. The height and attitude control system is controlled using a three-ring cascaded PID controller and an ADRC controller. Although the UAV's vertical height information is temporarily unreliable when it is interfered during the operation, our method can still ensure the stability of the aircraft. The EKF is used to predict the motion information of the drone, and the speed loop and the acceleration loop in the drone height control system are supervised to ensure the accuracy and controllability of the flight altitude during the autonomous cruise.

II. QUADROTOR RELATED MODEL DERIVATION

As seen in Fig. 1, P_i ($i = 1,2,3,4$) represents the position of the four power units of the quadrotor in the coordinate system. And in that coordinate system P_i can be defined as:

$$P_1 = [0 \quad 1 \quad 0]^T, P_3 = [0 \quad -1 \quad 0]^T,$$

$$P_2 = [1 \quad 0 \quad 0]^T, P_4 = [-1 \quad 0 \quad 0]^T.$$

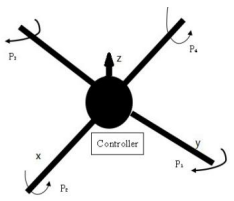

Figure 1. Structure diagram of the aircraft.

According to Newton's second law [10]:

$$F = ma = m\frac{dV}{dt}. \tag{1}$$

The overall motion velocity V relative to the ground of the quadrotor is decomposed into the velocity vector $\vec{V}$, that is $V = \begin{pmatrix} V_x & V_y & V_z \end{pmatrix}^T$ .And the motional equation of the quadrotor in the inertial coordinate system is as following:

$$F = ma = m\frac{d\vec{V}}{dt}. \tag{2}$$

where m represents the total mass of the quadrotor including its carrying peripherals; F is the resultant force the quadrotor received and consists of the gravity, the resistance, and the lift provided by the power unit of the quadrotor.

The direction of the quadrotor's gravity G is perpendicular to the z-axis, and G can be expressed as

$$G = \begin{bmatrix} 0 & 0 & -mg \end{bmatrix}^T. \tag{3}$$

The lift force is composed of four power units. The generating tension is proportional to the rotor speed of the power unit. The direction of the total tension N is perpendicular to the z-axis. The expression is as follows:

$$N_i = k_i \Omega_i^{\ 2}, \qquad i = 1,2,3,4 \tag{4}$$

Where

k_i ——the lift coefficient of the i rotor;

Ω_i ——the speed of the number i rotor.

Therefore, the total lift force N of the quadrotor is:

$$N = \begin{bmatrix} 0 & 0 & \sum_{i=1}^{4} P_i \cdot N_i \end{bmatrix}^T \tag{5}$$

The resistance of the quadrotor is mainly the air resistance during flight. The air resistance formula is:

$$F_s = \frac{1}{2} C\rho S V^2 \tag{6}$$

Where

C ——air resistance coefficient;

ρ ——air density;

S ——windward area of quadrotor ;

V ——quadrotor flight speed.

The resistance components of the quadrotor in all directions are as follows:

$$F = -\frac{1}{2} C\rho S|V|\vec{V}. \tag{7}$$

By the Eqs. (3), (4), (5), (6) and (7), we can obtain that

$$F = ma = \sum_{i=1}^{4} P_i \cdot N_i - mg - \frac{1}{2} C\rho S|V|\vec{V} \tag{8}$$

Supposing the angle of the pitching motion of the aircraft is θ, and the angle of the rolling motion is φ, and the angle of the yaw motion is ψ . In the geographic coordinate system Eq. (8) can be decomposed as:

$$\begin{cases} \ddot{x} = \frac{1}{m}(\sin\theta\cos\varphi\cos\psi + \sin\varphi\sin\psi)\sum_{i=1}^{4} P_i k_i \Omega_i^2 - \frac{C\rho S}{2m}\left|V_x^2\right| \\ \ddot{y} = \frac{1}{m}(\sin\theta\cos\varphi\cos\psi + \sin\varphi\sin\psi)\sum_{i=1}^{4} P_i k_i \Omega_i^2 - \frac{C\rho S}{2m}\left|V_y^2\right| \\ \ddot{z} = \frac{1}{m}\cos\theta\cos\varphi\sum_{i=1}^{4} P_i k_i \Omega_i^2 - \frac{C\rho S}{2m}\left|V_z^2\right| - g \end{cases} \tag{9}$$

It can be seen that the motion relationship between the motion of the aircraft in the inertial coordinates and the coordinate system of the aircraft is as shown by (9).

III. Design of Aircraft Self-stability Control Algorithm

The traditional cascade PID controller [11-13] is a typical linear controller. When PID controller is applied to the quadrotor UAV, a typical nonlinear control system, there will bring some inherent defects.RTK(Real - time kinematic) module can give the drone centimeter-level absolute positioning information in the inertial coordinate system, but it is easily interfered by the same frequency band information from the outside world, and the demanding to the surrounding environment is very high. It cannot be applied in buildings, water surfaces, etc. The interference of multipath effects makes the data unusable. When the absolute position information of the drone is damaged by the interference, the source of the position signal will be switched to the traditional spatial position sensor of meter-level.Its signal is poor and unstable, and the drone will shake quickly [14]. Therefore, ADRC (Active Disturbance Rejection Control) [15-16] algorithm is used to control the attitude of the UAV.A good control effect is obtained under the condition that the external disturbance is unknown.

The equation for the control system of the UAV can be obtained:

$$\begin{cases} dx_1 / dt = f_1(x_1) + x_2 \\ dx_2 / dt = f_2(x_1, x_2, t) + bu(t) \\ y = x_1 \end{cases} \tag{10}$$

where

x_1 ——angle data input;

x_2 ——angular velocity data input;

t ——time;

b ——system parameters;

$u(t)$ ——system nonlinear combination output;

y ——the final output of the system.

$f_1(x_1)$ and $f_2(x_1, x_2, t)$ are the system control functions and are known,and x_1 and x_2 can be measured. Using the state variable x_2 as the "virtual control variable" U_1 of the control state variable x_1, it is possible to set:

$$U_0 = U_1 - f_1(x_1) \tag{11}$$

Substituting (11) into (10) ,it can be rewritten as follows:

$$\frac{dx_1}{dt} = U_0 \tag{12}$$

The attitude loop of the UAV is composed of a pitch angle, a roll angle and a yaw angle.Due to the introduction of virtual control, the attitude loop can be divided into three independent channels and individually controlled by an unique corresponding virtual control variable.In order to facilitate the design of the controller and parameter tuning, the controller algorithms of the three attitude angle channels are the same and adopt the same parameters.Taking the yaw angle ψ channel as an example,The control algorithm is:

$$\begin{cases} \dot{v}_1 = v_2 \\ \dot{v}_2 = fhan(v_1 - v, v_2, r_0, h) \\ e = z_1 - y\psi \\ \dot{z}_1 = z - \beta_{11} e \\ \dot{z}_2 = z_3 - \beta_{12} fal(e, a_1, \delta) + b_0 u \\ \dot{z}_3 = -\beta_{13} fal(e, a_2, \delta) \\ e_1 = v_1 - z_1 \\ e_2 = v_2 - z_2 \\ u_0 = k_1 fal(e_1, a_1, c_0 h) + k_2 fal(e_2, a_2, c_0 h) \\ u = u_0 - z_3 / b_0 \end{cases} \tag{13}$$

where z_1, z_2, and z_3 are the output of the extended state observer (ESO) which estimates of the yaw angle x_1, the yaw angle differential x_2, and the yaw angle channel total disturbance x_3. β_{11}, β_{12}, β_{13} are the parameters that ESO needs to adjust. a_1, a_2 are adjustable parameters from 0 to 1. c_0, r_0, h, b_0 also are adjustable parameters. u is the system output. $fhan(\cdot)$ is the fastest control synthesis function.The specific algorithm is:

$$\begin{cases} d = rh^2 \\ \lambda_0 = hv_2 \\ y = (v_1 - v) + \lambda_0 \\ \lambda_1 = \sqrt{d(d + 8|y|)} \\ \lambda_2 = \lambda_0 + sign(y)(\lambda_1 - d)/2 \\ \lambda = (\lambda_0 + y) fsg(y, d) + \lambda_2 (1 - fsg(y, d)) \\ fhan = -r(\frac{\lambda}{d}) fsg(\lambda, d) - rsign(\lambda)(1 - fsg(\lambda, d)) \\ fsg(x, d) = (sign(x + d) - sign(x - d))/2 \end{cases} \tag{14}$$

And the $fal(\cdot)$ function formula is:

$$fal(e, a, \delta) = \begin{cases} |e|^a sign(e), |e| > \delta \\ \dfrac{e}{\delta^{1-a}}, |e| \le \delta \end{cases} \tag{15}$$

The general block diagram of the algorithm is as follows:

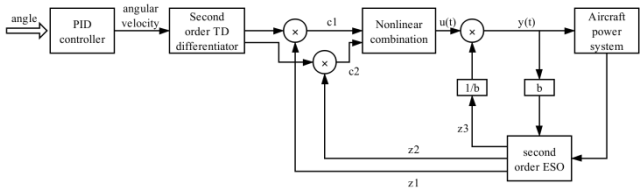

Figure 2. ADRC algorithm flowchart.

IV. AIRCRAFT HEIGHT CONTROL ALGORITHM DESIGN

Fully autonomous flying drones work mostly on cruise routes, which requires a stable flight height to ensure it works stably. Therefore, the flight of the aircraft needs to be more reliable and safe through a height control algorithm [17].The Extended Kalman filter was developed for nonlinear discrete-time processes [18-19] using a two-step predictive correction algorithm. The first step involves estimating the latest state estimate and the estimate of the error covariance to calculate a predicted estimate of the current state. The second step corrects the predicted state estimate calculated in the first step by combining the most recent process measurements to generate an updated state estimate.

Since height sensors (e.g., barometer) generally have phenomena (such as temperature drift), the height, height speed, height acceleration, and the corresponding error of the three are taken as observations, wherein the aircraft height and the height acceleration can be directly obtained by the sensor, and the height speed can be obtained by the two [20]. Therefore, the observed variable can be written as:

$$X(k) = [Z_1(k) \quad Z_2(k) \quad Z_3(k) \quad b_1(k) \quad b_2(k) \quad b_3(k)]^T. \tag{16}$$

where

$b(k)=[b_1(k)\quad b_2(k)\quad b_3(k)]^T$ ——Height data error, height velocity data error, height acceleration data error;

$Z_1(k)$——Aircraft altitude;

$Z_2(k)$——Aircraft altitude speed;

$Z_3(k)$——Aircraft altitude acceleration.

We can express the aircraft altitude Extended Kalman filter prediction algorithm as follows:

1) System state estimation

$$\hat{X}(k+1|k)=\hat{X}(k|k)+f[\hat{X}(k|k)]\Delta t + A[X(k|k)]f[\hat{X}(k|k)]\frac{(\Delta t)^2}{2}. \quad (17)$$

where

$$A[X(k)]=\left.\frac{\delta f}{\delta X}\right|_{X=X(k)}. \quad (18)$$

$f[\cdot]$ is a general-purpose multidimensional vector function.

2) a priori error covariance matrix

$$P(k+1|k)=\Omega(k)P(k|k)\Omega^T(k)+Q(k) \quad (19)$$

Where

$$\Omega(k)=I_{6\times 6}+A[\hat{X}(k|k)]\Delta t, \quad (20)$$

$$Q(k)=E[W(k),W(k)^T]. \quad (21)$$

3) Calculating Kalman gain

$$K(k+1)=P(k+1|k)H^T(k+1)\cdot [H(k+1)P(k+1|k)H^T(k+1)+R_{k+1}]^{-1}. \quad (22)$$

where

$$H(k+1)=[I_{4\times 4}\quad 0_{4\times 3}] \quad (23)$$

$$R(k)=E[V(k),V(k)^T] \quad (24)$$

4) Posterior state estimation

$$\hat{X}(k+1|k+1)=\hat{X}(k+1|k)+K(k+1)\cdot \{Z(k+1)-h[\hat{X}(k+1|k)]\} \quad (25)$$

5) Update error covariance matrix

$$P(k+1|k+1)=[I-K(k+1)H(k+1)|P(k+1|k)] \quad (26)$$

B. High Cascade PID Controller

After the sensor data is filtered and predicted by the Extended Kalman filter, it is then necessary to add this data as input to the high-level three-loop cascade PID controller for control. The single-ring PID separately performs PID calculation on a set of feedback and input and outputs control signals to the motor.However,the control quality of the single-loop PID is poor. To further increase the anti-interference ability and damping of the system, it is necessary to introduce cascade PID control.

The traditional PID controller consists of proportional, integral, and derivative terms. If the controller output is $u(k)$, then:

$$u(k)=K_p e(k)+K_i\sum_{n=0}^{k}e(n)+K_d(e(k)-e(k-1)). \quad (27)$$

where $e(k)$ is system input, K_p, K_i and K_d is proportional, differential, integral parameters. The schematic diagram of the cascade PID controller is as follows:

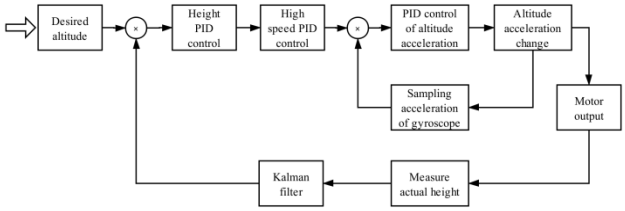

Figure 3. Controller schematic of three-ring cascade PID.

The height controller is a PD controller that controls the amount of altitude error and uses the output as an input to the height speed controller. The height speed controller performs error control on it, and the output result is input to the height acceleration controller and finally output to the motor.

V. TEST RESULTS

In order to verify the effectiveness of the system, the quadrotor and the super-signal interference source were tested. The test hardware platform is shown in Fig.4.

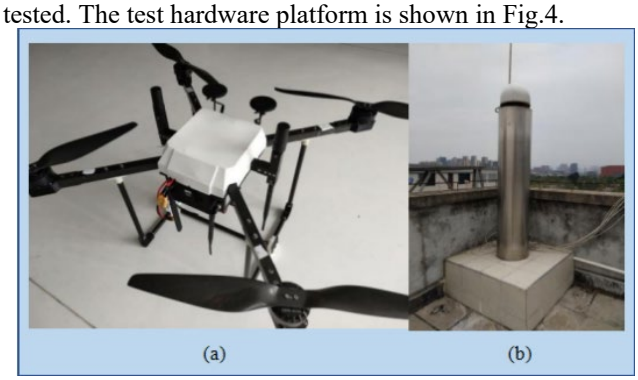

Figure 4. UAV(a) and interference source(b).

A. *Extended Kalman filter test*

The altitude data source of the aircraft mainly includes the ultrasonic module and the barometer module. When the aircraft performs the mission at a height close to the ground, the altitude algorithm uses the data of the ultrasonic module; When the flight altitude is high, the barometer is used. The height data obtained from the height sensor needs to be filtered and predicted by the designed Extended Kalman filter to become usable height data.

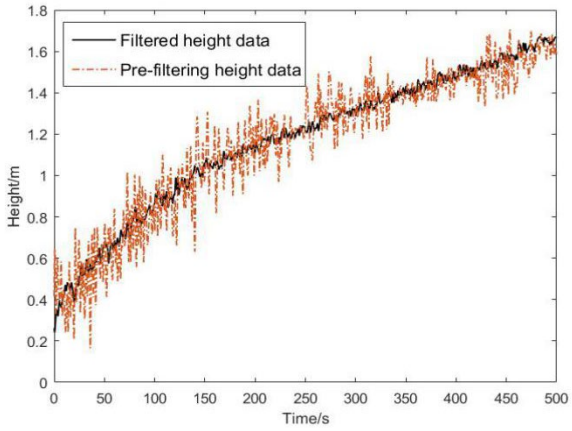

Figure 5. Height data before and after filtering.

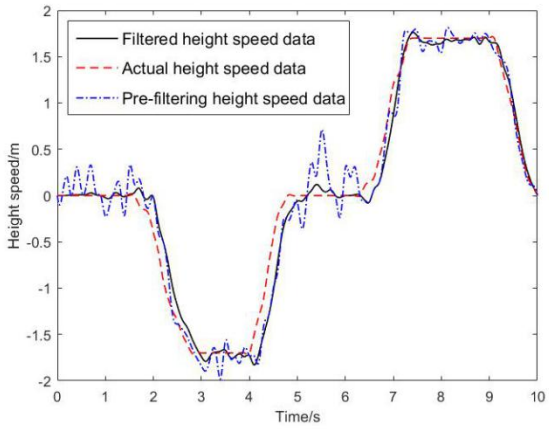

Figure 6. High speed data before and after filtering.

In order to test the influence of interference on the drone, the device emits a passband interference at 12.5s. Seeing from Fig. 5 ,although the changes of the trend of unfiltered and filtered height data changes are the same, since the variance of the unfiltered height data is too large.That is not suitable for the next height control, especially in the interference zone, the data was clearly lost. Although the height data after Extended Kalman filtering will also be jittery, the jitter is not large and the curve is smooth, which can be used as the input of the next control algorithm.The test results of height speed are shown in Fig. 6.

The Extended Kalman filter can filter the height data and is more effective than other data filtering techniques (such as complementary filtering). The height data obtained by the complementary filtering is similar to the data obtained by the Extended Kalman filter, but there is a significant phase delay. As shown in Fig. 5, if the height data is not filtered at all, the obtained height data is extremely jittery, and the aircraft can not only be fixed in height but also crashes directly, Therefore, we can only use the different height determination schemes of complementary filtering algorithm and Extended Kalman filtering algorithm.

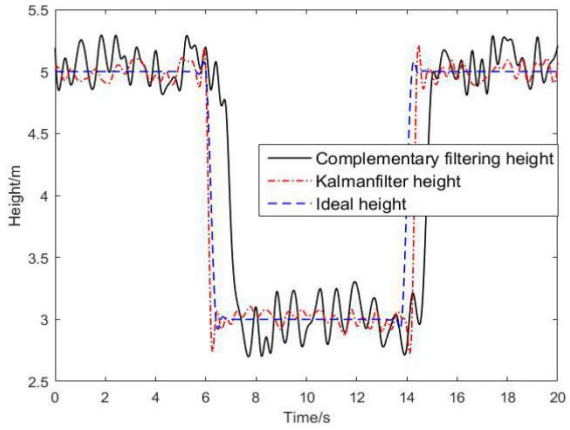

Figure 7. Reference ideal height curve.

It can be seen from Fig. 7 that the Extended Kalman filter has less time delay and the data variance is smaller than that of the complementary filtering, and the complementary filtering algorithm has poor data followability.

B. *ADRC Control Algorithm Test*

At the same time, in order to better control the attitude of the aircraft during the cruise process, it is guaranteed that the anti-interference algorithm does not lose the fast response capability of the system. In the test, the angle θ of the pitch motion is taken as an example.Comparing the test results of cascade PID control with ADRC algorithm control (assuming the desired deflection angle is 5 degrees, initially 0 degrees). The test results are shown in Fig 8:

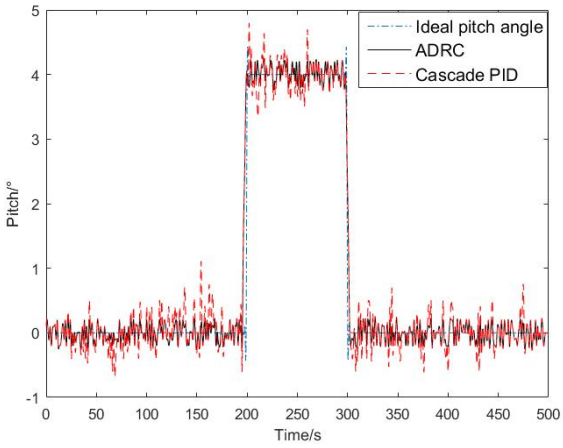

Figure 8. Flight attitude test chart under different algorithms.

From Fig. 8 it can be seen from the figure that under the strong interference, the traditional over-modulation of the cascade PID controller is no longer suitable for the attitude control of the aircraft, and the interference of the sudden noise in the environment leads to a sudden change of the attitude of the aircraft. Although it is still possible to adjust back to the normal desired posture, the jitter is noticeable. The ADRC algorithm can ensure that there is no overshoot in the aircraft, and the error range of the attitude control is within a reasonable and controllable range.

VI. CONCLUSION

A. By adopting the control method combining the ADRC (Active Disturbance Rejection Control) controller and the PID controller, the drone can obtain better control effects.

B. For designing the auto-disturbance controller, the tracking differentiator is used to obtain the differential signal from the controlled object, and then the nonlinear expansion observer is used to realize the disturbance estimation and compensation. Finally, the proportion quantity, differential quantity and integral quantity of the errors are combined nonlinearly.

C. In order to enhance the anti-interference ability of the system, the Extended Kalman filter is used to predict and process the altitude data that the sensor receives, and the cascade PID is introduced to control the flight attitude of the drone within a reasonable range.

The algorithm proposed in this paper has good robustness, but in some extreme environments, there are still some shortcomings. In the future, we will be committed to introducing vision module into the navigation of UAV, and further expand the application scenarios and anti-interference capabilities of UAV.

ACKNOWLEDGMENT

I would like to thank Fuzhou University for its concern, support and help to this paper. At the same time, I would like to thank the scholars of this paper for their monographs.

REFERENCES

[1] Li Weijiang. Research Status and Trends of Agricultural Plant Protection UAVs [J]. Agriculture and Technology, 2018(10).

[2] He Yong, Xiao Shuzhen, Fang Hui, et al. Development status and application decision of plant protection drone spraying nozzle[J]. Transactions of the Chinese Society of Agricultural Engineering, 2018, 34(13): 113-124.

[3] Wu Di, Li Junxing, Yuan Hongyin. Research Status of Low-altitude Low-volume Spray Technology for Plant Protection UAV[J]. Agriculture & Technology, 2018(1): 45-47.

[4] Wang Dashuai, Zhang Junxiong, Li Wei, Xiong Bin, Zhang Shunlu, Zhang Wenqiang.Design and Experiment of Dynamic Variable Application System for Plant Protection UAV[J]. Transactions of the Chinese Society of Agricultural Machinery, 2017, 48(5): 86-93.

[5] Zhai Jiayu, Qi Hailong. Design of autonomous takeoff and landing system for locomotives with cascade PID[J]. Automation and Instrumentation, 2010, 25(10): 28-33.

[6] Ma Xu, Cheng Yumei, Hao Shuai. Adaptive S-Filtering Method for Highly Fusion Estimation of UAV[J]. Chinese Journal of Inertial Technology, 2013, 21(5).

[7] Tian Yong, Li Tian, Cai Yunpeng. A Method for Designing the Residual Sensor Height of Small Unmanned Aerial Vehicles[J]. Journal of Shenyang University of Technology, 2012(3):349-353.

[8] Wu Kaihua, Sun Xuechao, Zhang Jingcheng, et al. Research on imitation flight method of plant protection drone based on high fusion[J]., Journal of Agricultural Machinery.

[9] Welch G, Bishop G. An Introduction to the Kalman Filter[J]. 1995, 8(7):127-132.

[10] Isaac Newton. The Mathematical Principles of Natural Philosophy [M]. Shaanxi People's Publishing House, 2001.

[11] Yang Zhi, Zhu Haifeng, Huang Yihua. Overview of PID Controller Design and Parameter Tuning Methods[J]. Chemical Industry Automation and Instruments, 2005, 32(5): 1-7.

[12] Feng Qingduan, Qi Hailong. Application of Cascade PID Control in UAV Attitude Control[J]. Microcomputer Information, 2009, 25(22): 9-10.

[13] Ding Jun, Xu Yongwei. Single Neuron Adaptive PID Controller and Its Application[J]. Control Engineering, 2004, 11(1): 27-30.

[14] Su Yuxin, Duan Baoyan. A Novel Nonlinear PID Controller[J]. Control and Decision, 2003, 18(1): 126-128.

[15] Pu Jun, Han Jingqing. Simulation Software of Active Disturbance Rejection Controller (ADRC)[J]. Journal of System Simulation, 1999(5): 383-387.

[16] Zhong Haixin, Lu Qian, Qiu Senhui, et al. Attitude control of quadrotor UAV based on ADRC[J]. Journal of Jiangxi Normal University(Natural Science), 2017, 41(1): 67-72.

[17] Wu Kaihua, Sun Xuechao, Zhang Jingcheng, Chen Fengnong.Study on the Imitation Flight Method of Plant Protection UAV Based on High Fusion[J]. Transactions of the Chinese Society of Agricultural Machinery, 2018, 49(6): 17-23.

[18] Wan Qin, Wang Yaonan. Motion Target Detection and Tracking Based on Kalman Filter[J]. Journal of Hunan University(Science & Technology), 2007, 34(3): 36-40.

[19] Peng Dingcong. Basic Principles and Applications of Kalman Filtering[J]. Software Guide, 2009(11): 32-34.

[20] Hu Guorong, Ou Jikun. Improved High Dynamic GPS Positioning Adaptive Kalman Filtering Method[J]. Acta Geoda Sinica, 1999, 28(4): 290-294.